Available online at www.sciencedirect.com

ScienceDirect

Procedia Computer Science 180 (2021) 200–207

Procedia Computer Science

www.elsevier.com/locate/procedia

International Conference on Industry 4.0 and Smart Manufacturing

Sensor Shirt as Universal Platform for Real-Time Monitoring of Posture and Movements for Occupational Health and Ergonomics

Phillip Petz[a], Florian Eibensteiner[a], Josef Langer[a]

[a] *University of Applied Sciences Upper Austria, Embedded Systems Lab, 4232 Hagenberg, Austria*

Abstract

With the continuing development in integrating electronics into textiles in the field of smart textiles and wearables, new innovations for monitoring the human environment and new possibilities for human-machine interaction are constantly emerging. Depending on the type of sensor technology used, monitoring human motion and its environment allows applications in various fields, like occupational safety, protection and rehabilitation in the form of protective work clothing. In this paper the development of a sensor shirt is described, which records the movement and position of the upper body by several inertial sensors and transmits the sensor values via Wi-Fi. Based on the developed prototype, this paper shows the typical problems in the development of intelligent clothing and presents possible concepts which can be implemented already in the design phase. First measurements of the prototype show the potential of the shirt as well as possible future applications in the field of occupational safety and human-machine interaction.

© 2021 The Authors. Published by Elsevier B.V.
This is an open access article under the CC BY-NC-ND license (https://creativecommons.org/licenses/by-nc-nd/4.0)
Peer-review under responsibility of the scientific committee of the International Conference on Industry 4.0 and Smart Manufacturing

Keywords: smart textiles; human-machine interaction; occupational health and safety; ergonomics

1. Introduction

Because of their flexible properties and their natural proximity to the human body, textiles are a protective layer against environmental influences. Starting with the preservation of body heat, textiles are now able to ward off mechanical stress, chemical influences or even radiation. The next step in the development of textiles is the connection with electronics and enables all existing types of textiles, sensor and motor applications to be expanded in the immediate human environment. The first concepts to connect conductive elements with textiles have been around since the middle of the 19th century, with copper wires and other conductive metal strands being interwoven with textiles in the manufacturing process . This connection was primarily intended to adapt the mechanical properties of the textile

* Corresponding author. Tel.: +43-5-0804-27146 ; fax: +43-5-0804-22499.
E-mail address: phillip.petz@fh-hagenberg.at

1877-0509 © 2021 The Authors. Published by Elsevier B.V.
This is an open access article under the CC BY-NC-ND license (https://creativecommons.org/licenses/by-nc-nd/4.0)
Peer-review under responsibility of the scientific committee of the International Conference on Industry 4.0 and Smart Manufacturing
10.1016/j.procs.2021.01.157

instead of providing the textile with conductive qualities. At that time, a greater expansion failed due to the high demands on the manufacturing process and the low benefit for conductive textiles. With the invention of transistors, these conductive elements could finally be used, as not only energy, but information was able to be exchanged within the textile. Such smart clothes utilize either conventional wires, which are stitched or laid in the textile, or newer methods of coating threads and fabrics with a conductive mantle. While the use of solid electrical conductors makes transmission simpler and easier, the requirements for washability and simultaneous flexibility of textiles hinder the application possibilities of most implementations. [7] showed with their intelligent undershirt that it is possible to classify occupational manual material handling tasks using sensors worn on the body. For the smart undershirt, eleven textile tension sensors were distributed on the back and arms. The patches were connected to a pcb on the back, from which the data was transferred via cable to a PC. The classification of movements allowed the classification of occupational manual material handling tasks. This classification and detection enables ergonomic exposure assessment systems and helps prevent occupational injuries. [5] developed a sensor node with integrated textile sensors. Conductive threads in the shirt are used as electrodes in order to be able to make statements about the state of health of a test person based on ECG data and values from an acceleration sensor. The shirt only uses a single node and any data that is collected is transmitted directly from the node to a base station via Bluetooth.

In the work of [9], scientists from the Massachusetts Institute of Technology have developed a sensor shirt that uses flexible and coated conductive tracks for energy and information transfer in the shirt. These meander-shaped tracks are divided into short island segments and can be arranged in any combination depending on the application. Two dedicated lines are available for data transmission, which are used for communication with I2C. Since, this form of transmission requires fixed addresses for the sensors, only sensors that can adapt their address by external circuitry can be used. Furthermore, only one sensor at a time can be read out by connecting it to a bus topology. Once the combination of connection islands and sensor islands in the shirt is selected, this sequence and sensor type cannot be changed later. The resulting network is then soldered, coated and placed in tubes in the shirt. A removable ub acts as a Gateway and then streams the sensed values over Bluetooth to an external device. Although, there are already several different systems for the recognition and classification of posture, movement and load, no system is yet mobile and at the same time flexible in its application and use case. In this paper we present a new textile sensor shirt, which can be used to record posture and movement sequences and can be easily customized. Especially the quick adaptability of modular sensor nodes allows our shirt to perform varying sensing scenarios and evaluations as a universal measurement platform.

2. Wearable Sensor Shirt System

The sensor shirt has eight distributed sensor positions, which are in the neck and shoulder area, on the upper and lower arms, and in the area of the lumbar vertebrae. Another sensor node can be positioned in the area of the hip, which in our prototype is also used for data transmission in addition to data recording. This node is equipped with Wi-Fi and Bluetooth capabilities and provides the power supply for the shirt. The individual sensor nodes, as well as the node for data transmission, can be removed for washing. The nodes are connected to the shirt with 9 mm snap fasteners. The positions in the shirt are predetermined for a given shirt as the individual snaps are connected with conductive stainless steel filament yarns. The yarns have a resistance of 63 $[\frac{\Omega}{m}]$. In Fig. 1 the positions of the several sensor nodes, marked with brown rectangles, are shown.

2.1. Individual Sensor Nodes

The sensor nodes are responsible for measuring motion or environmental data and can also pre-process these data. Each node can therefore either use standalone sensors or its own microcontroller, which additionally can be connected to various other types of sensors. The node electronics, which were used for collecting the motion data, consists of a STM SensorTile board, which contains a Cortex M4F microcontroller with external accelerometer, gyroscope, magnetometer, humidity and pressure sensors. It has a built-in low dropout voltage regulator to supply these components. Tab. 1 summarizes the specifications of the sensor node used for the motion detection tests.

The SensorTile is soldered onto an adapter board which uses conventional 9 millimeter snap fasteners to connect to the textile. The positions of the two lower snap fasteners are shifted closer to each other, thus false connection to the

Fig. 1. Position of sensor nodes.

Table 1. Specification of first sensor node.

Device	Specification Item	Specification
Microcontroller	Model Number	STM32L476JG
	Frequency	80 MHz
	Flash Memory	1 MB
	RAM Memory	128 kB
Accelerometer & Gyroscope	Model Number	LSM6DSM
	Dimensions	3-axis
	Resolution	16 Bit
	Sampling Rate	100 Hz
Magnetometer	Model Number	LSM303AGR
	Dimensions	3-axis
	Resolution	16 Bit
	Sampling Rate	100 Hz

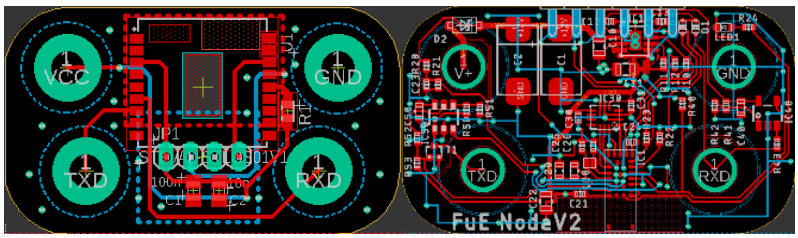

Fig. 2. (a) Schematic of STM node; (b) Schematic of Nordic node.

shirt is prevented. The SensorTile is mounted in the center on the backside of the board. Instead of the ST SensorTile other microcontrollers and sensors can be used as well. The only requirement that must be met for expansion is the format and layout of the snaps in the pockets of the shirt. Fig. 2 shows a layout for an adapter board with a Nordic microcontroller and external sensors as an alternative to the STM Controller. A value of 100 Hz was chosen for the sampling rate in order to record posture and movement in an energy-efficient manner without any major loss of accuracy. The influence of the sampling rate in the detection of parameters during the run was investigated in [6]. The running motion on a treadmill at 13 kmh of 21 male subjects was recorded at 1000 Hz and reduced to lower sampling rates in post-processing. For heel acceleration, a sampling rate of 200 Hz was determined to be the minimum data rate for a small error. Since there are no further investigations of the sampling rate and accuracy of upper body movements, a maximum speed of 6 kmh and a sampling rate of 100 Hz was used for the upper extremities.

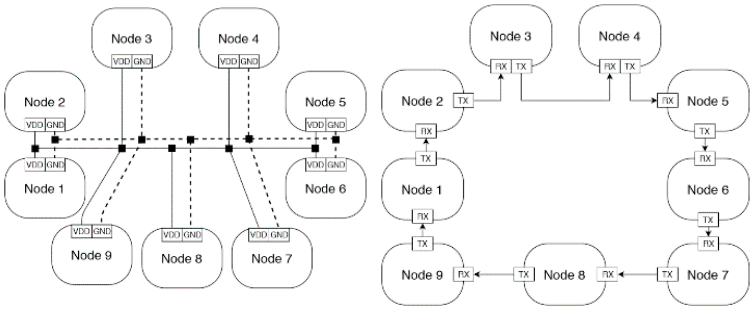

Fig. 3. (a) Bus topology for power transmission; (b) Serial link ring topology for data transmission using UART.

2.2. Energy and Data Transfer

Two conductive stainless steel-yarns are stitched to all nodes in a meander pattern for energy transmission. For data transmission, additional conductive yarns were stitched between the transmit connection and the receive connector from the following sensor node. Thus, each node has four connections, two for the supply voltage, and ground, and two for receive and transmit data. By physically separating the data line into two connections, the shirt supports bus topologies such as single wire and at the same time a serial link ring structure with UART(Universal Asynchronous Receiver Transmitter). Mixing up both topologies is also technically possible within a single shirt, since the connection type and topology are ultimately defined by the PCB layout of the neighbouring nodes. Fig. 3 shows the topology of the power supply as bus and the communication as serial link ring structure. This type of connection has also been used to record the movement datasets used in this work. UART was chosen for transmission because this communication method is easy to implement and can be used in an energy-saving manner without the need for an additional clock line.

3. Measurements

Initial measurements on the electrical behaviour of the conductive yarns in the shirt have shown that the textile has a high resistance in conjunction with the contact resistance of the press studs. This resistance of up to 50 Ω between nodes affects the data lines as well as the power supply and ground, which causes the voltage level of the logical ’1’ to decrease and the voltage level of the logical ’0’ to increase. For data transmission, long cable lengths or low voltage levels can, therefore, lead to mis-interpretations in the receiver. If the behaviour and the connection itself are known in advance, the appropriate voltage level for the data line can be created for the receiving node by adding an op-amp to the input line of the node. Due to the high line resistances, we also measured an increased energy demand in the node and voltage drop on the supply line during active data transmission. The energy required for data transmission at a given resistance is provided in by back-up capacitors at the individual nodes. In doing so, energy loss on the supply lines can be kept to a minimum due to the cyclical data transmission. Our current measurements of the nodes have shown that an additional 50 mA flows via the supply line due to the transmission of all 96 data bytes. At 38,400 Baud, additional energy is, therefore, required for 17.5 ms. The ratio of current, charge and time in Equation 1 was used to determine the size of the backup capacitor to be 220 µF.

$$I[A] = \frac{C[F] \cdot U[V]}{t[s]} \tag{1}$$

Furthermore, the amplitude response and the frequency response of the textile cables were determined for maximum data transmission. A function generator feeds a sinusoidal signal with a defined frequency into the first channel of an oscilloscope and into the textile transmission channel. At the end of the transmission channel, the signal is fed into the second channel of the oscilloscope. For the Bode diagram, the peak-to-peak voltage and the phase offset are measured on the oscilloscope. Since the attenuation is 3 dB starting at 2 MHz, this paper will not go into the behaviour of the textiles at higher frequencies in more detail in respect of the 38,400 Baud rate used for data transmission.

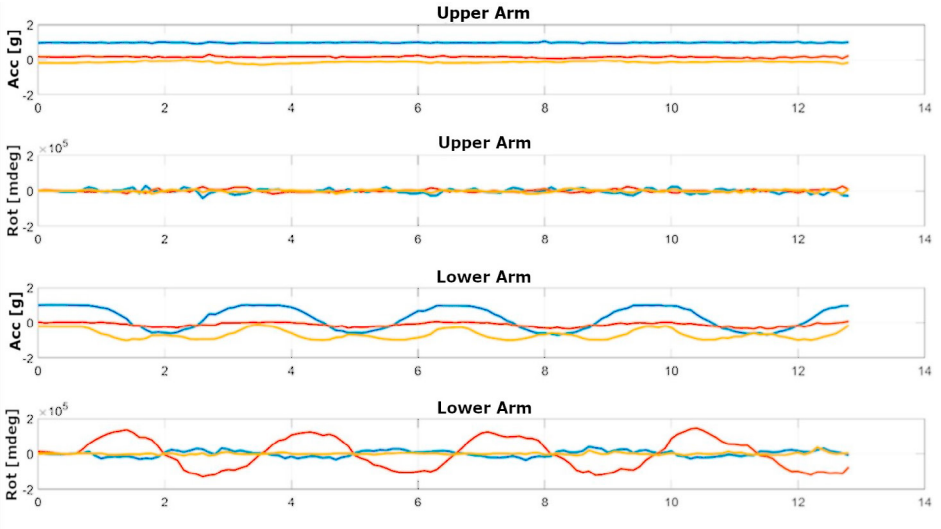

Fig. 4. Visualization of accelerometer and gyroscope data during flexion and extension of the forearm.

3.1. Simple Movements

The linear acceleration forces and rotational speeds of the individual sensors in all three axes were used to measure the movement. The data is transmitted by UART working at 38400 Baud using the token ring network. For the first analysis of the sensor system, simple movements were defined and the measured results of the several sensors were compared to each other. The first test included flexion and extension of the forearm over several repetitions. With these simple movements, the speed of the movement and the number of repetitions can already easily be read without filtering and pre-processing the data. The course of rotation and linear acceleration for this test is shown in Fig. 4. The three lines of each plot represent the measured values for each axis for acceleration and rotation separately. The first two plots visualize the sensors of the upper arm, the lower two plots the forearm during extension and flexion. While doing the flexion and extension test, all other sensors are not affected. Therefore, for the analysis of this simple movement, it is sufficient to estimate a single sensor node for evaluation of position and movement of the forearm.

For the following refinement of the data and determination by algorithms, a moving mean filter with a window size of 5 is used, which is sufficient due to the low speed of the movements. [8] have shown that the choice of cutoff frequency for a low pass filter for human motion can be arbitrary as long as the first Nyquist condition is not violated.

3.2. Posture Recognition

The second test examined how well different postures can be differentiated by the provided nodes. For this purpose, three positions ‘leaning back’, ‘straight’ and ‘leaning forward’ were defined and held for 5 seconds or 50 data samples. The stationary postures with the test person are shown in Fig. 5. As the arms are not responsible for the measured posture of the back, only the sensors on the spine and the shoulders were measured. The orientation of the coordinate systems of the used sensors are all aligned in a plane parallel to the back. The acceleration is most noticeable on the X-axis of the sensors in an upright position. The Z-axis acts out of the body plane, while the Y-axis runs along the shoulders. Since, only gravity acts on the axes of the sensors at rest, the distribution of the constant accelerations can be used to determine the orientation in space. Through the orientation of the sensors, the rounding of the back can be determined in a further step. The measured values of the tests were averaged for this purpose and the variance of the individual axes and sensors were determined. The division of the forces into X, Y and Z allows the representation in a 3D coordinate system. Fig. 5 shows the distribution of the sensor values at different positions graphically.

This figure illustrates the distribution of the acceleration across the three dimensions at the given positions. The colour of the surfaces and corner points indicate the examined position. The green values represent the forward leaning posture, the red values represent the straight sitting posture, and the blue values are from the measurement with the

Fig. 5. (a) leaning on the backrest; (b) sitting straight; (c) front over bent.

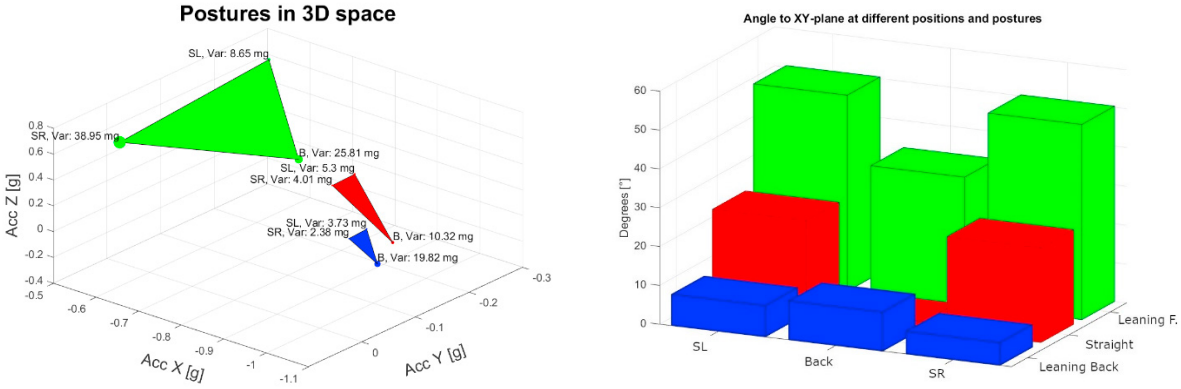

Fig. 6. (a) Distribution of measured acceleration across the three axes for examined postures; (b) Angles for different sensor positions and postures related to XY-plane.

leaning posture. The corner points represent the averaged values of the axes of the sensors on the left shoulder (SL), the right shoulder (SR), and the back (B). The visualization of the corner points uses the greatest variance among the three axes of a sensor as radius. In our measurements, the variance of the other axes was significantly lower during the same measurement. The visualization of the maximum variance in a corner point will be interpreted as worst case representation. The connection of the points in space leads to new planes, where the area of the triangle illustrates the similarity between the sensor values. It is noticeable that the resulting plane has by far the largest surface area when the body is leaning forward. This is explained by the curvature of the back when the posture is bent forward, which considerably diverges the representative points of the shoulders along the Y-axis. The upright and leaning positions share more similarities in relation to shoulders and back. To determine the posture, the angle between the individual points and the origin, as well as a point in relation to the XY plane can now be determined via dot product and the division by the product of the vector magnitude from the position in the coordinate system. In the following, Fig.6 shows the determined angles of the position from Fig. 5 as a function of the posture and sensor position. The colours correspond to the postures from Fig. 5.

The most significant angles determined are summarized in Table 2. ∠BSL and ∠BSR are the respective angles, which are spanned from the coordinate from the spine sensor B to the coordinate of the left and right shoulder sensors SL and SR. The discrepancy between these angles is defined by ΔSLSR. Finally, the angle between the shoulders ∠SLSR is determined.

3.3. Detection of more complex motions

In addition to the detection of basic motions with isolated sensors or the posture in stationary sections, statements about complex processes can also be made. In order to be able to perform such motion sequences in a repeatable

Table 2. Posture dependent angles.

	Straight	Bent	Leaning
∠BSL	22.3320°	17.4360°	-1.9665°
∠BSR	22.6058°	17.2347°	-4.1648°
ΔSLSR	0.2738°	-0.2013°	-2.1982°
∠SLSR	2.8337°	28.4575°	1.3323°

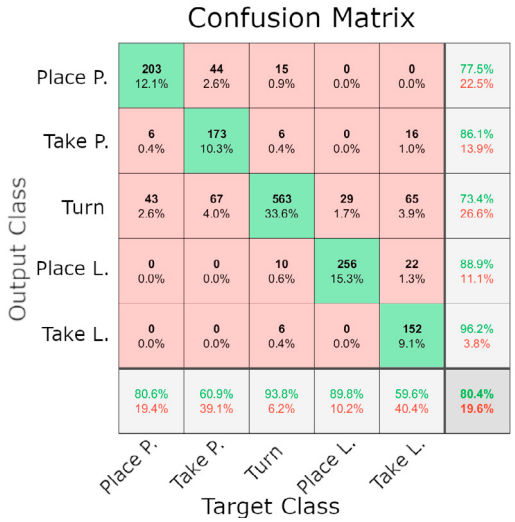

Fig. 7. Confusion matrix for chosen movements after classification by LSTM model.

manner, a test environment was set up to flexibly test the movements 'rotate', 'take parcel from desk', 'place parcel on desk', 'take parcel from shelf' and 'place parcel in shelf'. The rotation of 180 degrees can be done in both directions and the parcel can be placed in one of five compartments of the shelf. A `C#`-Application was written to record the data and coordinate the measurements. The measurement sequence is structured by voice command in time slots of 3 seconds and the measured values are stored with labels in a CSV file. All movement sequences were recorded several times during a test and performed at different speeds. To detect overfitting and underfitting, the data was divided into four parts training data and one part verification data. The training data was then used to train an LSTM model to detect the movements. The parameters of the model used are shown in Table 3.

Table 3. Parameters for LSTM Model.

Training / Verification Size	6030 / 670
Predicted Classes	5
State Activation Function	tanh
Gate Activation Function	Sigmoid
Gradient Threshold Norm	L2
Solver for training	adam

The model used consists of an input and classification layer, as well as an LSTM layer, a connection layer, and a softmax layer. The model was trained for 11 epochs, as training for more iterations lead to overfitting and worse results in verification. An accuracy of above 80% was determined with the original verification dataset. The resulting confusion matrix using this model is shown in Fig. 7. With PlaceParcel and TakeParcel, the box is placed on a table, while PlaceLevel and TakeLevel place the box in any compartment of the shelf. Fig. 7 shows that the motion sequences can be well identified by an LSTM model. As an alternative, a GRU layer was also used instead of the LSTM layer, but the performance of the model remained the same.

4. Conclusions

We have introduced a T-shirt with conductive textile yarns, which can be equipped and interchanged with any type of sensors via push buttons. By measuring the energy consumption in each node, the size of the supporting capacitors can be determined and the resistances of the textile conductors, which are comparatively high in comparison to conventional conductors, can be overcome. The use of different sensors allows a quick adaptation to new requirements in measurement and detection of human motions. Which sensors are later used in a shirt are not important for the manufacturing process of the shirt. Only the number and position of the sensor nodes must be defined at the beginning. Furthermore, the design offers the possibility of a designated microcontroller on each sensor position. Thus, the detection of different positions and movements can be done in the shirt and does not require any further transmission to a host computer for processing. Data analysis and interpretation can be done via simple decision trees or proprietary machine learning algorithms suited for microcontrollers and calculation directly on the nodes. By using acceleration and rotation sensors, it was shown that a comprehensive motion and posture image can be created using distributed sensors. In creating an LSTM model and data post-processing, it was possible to classify the learned motion sequences with an accuracy of above 80%. A more detailed analysis of the data can provide further information about connections in the acquired data, and further, reduce the calculation effort in each sensor node by reducing redundant information.

With the movement and posture detection and recognition, measurement and monitoring of the biomechanical load as well as repetitive actions is possible. These data can be crucial in detecting diseases such as musculoskeletal disorders [1] in advance and avoid them through preventive measures. Approaches for such measurements and integration into simulations with a digital twin were presented in [2] and [3], among others. Besides the recognition and evaluation of posture and movement under the aspect of ergonomics, the presented shirt can also be used to make a statement about the efficiency and distribution of work on assembly lines in real time. In [4] a methodical framework was presented, which allows portable sensors and simulation tools for the analysis of performance parameters and work distribution in the field of industrial engineering. The measurement systems for recording posture and classifying the work steps presented were based either on the separate attachment of sensors with power supply and data transmission to the body or on the creation of a complete suit with a distributed sensor network. Due to the flexibility in positioning and sensor type given by the design and structure of the sensor shirt, measurement concepts can be created, revised and refined for initial investigations as well as for more detailed studies. Our sensor system can therefore be used as a universal platform for recording and classifying movement sections for ergonomics analyses, work and movement sequences or workflows.

References

[1] Alessio, L., Franco, G., Tomei, F., 2015. Trattato di medicina del lavoro. Piccin Nuova Libraria.

[2] Caputo, F., D'Amato, E., Greco, A., Notaro, I., Spada, S., 2018a. Human posture tracking system for industrial process design and assessment, in: International Conference on Intelligent Human Systems Integration, Springer. pp. 450–455.

[3] Caputo, F., Greco, A., D'Amato, E., Notaro, I., Sardo, M.L., Spada, S., Ghibaudo, L., 2018b. A human postures inertial tracking system for ergonomic assessments, in: Congress of the International Ergonomics Association, Springer. pp. 173–184.

[4] Fera, M., Greco, A., Caterino, M., Gerbino, S., Caputo, F., Macchiaroli, R., D'Amato, E., 2020. Towards digital twin implementation for assessing production line performance and balancing. Sensors 20, 97.

[5] Lee, Y.D., Chung, W.Y., 2009. Wireless sensor network based wearable smart shirt for ubiquitous health and activity monitoring. Sensors and Actuators B: Chemical 140, 390–395.

[6] Mitschke, C., Zaumseil, F., Milani, T.L., 2017. The influence of inertial sensor sampling frequency on the accuracy of measurement parameters in rearfoot running. Computer Methods in Biomechanics and Biomedical Engineering 20, 1502–1511. URL: https://doi.org/10.1080/10255842.2017.1382482, doi:10.1080/10255842.2017.1382482, arXiv:https://doi.org/10.1080/10255842.2017.1382482. pMID: 28948846.

[7] Mokhlespour Esfahani, M.I., Nussbaum, M.A., Kong, Z., 2019. Using a smart textile system for classifying occupational manual material handling tasks: Evidence from lab-based simulations. Ergonomics 62, 823–833.

[8] Schreven, S., Beek, P.J., Smeets, J.B., 2015. Optimising filtering parameters for a 3d motion analysis system. Journal of Electromyography and Kinesiology 25, 808–814.

[9] Wicaksono, I., Tucker, C.I., Sun, T., Guerrero, C.A., Liu, C., Woo, W.M., Pence, E.J., Dagdeviren, C., 2020. A tailored, electronic textile conformable suit for large-scale spatiotemporal physiological sensing in vivo. npj Flexible Electronics 4, 1–13.